Table 1. Rhenium labeling using the solid-supported hydrazine **4**.

Entry	Concentration [10^{-5} M]	Conditions[a]	Time [h]	Yield [%]
1	2	A	2	53
			5	72
2	0.2	B	2	50
			5	70
3	9.3	C	2	54
			5	70
4	2	D	2	55
			5	65

[a] Reactions carried out in CH_2Cl_2 (10 mL) at 40 °C. Reactant ratios used: A: **4**/PPh_3/$[ReOCl_3(PPh_3)_2]$ = 100/100/1; B: **4**/PPh_3/$[ReOCl_3(PPh_3)_2]$ = 1000/1000/1; C: **4**/PPh_3/$KReO_4$ = 100/100/1; D: **4**/$HPPh_3Cl$/Bu_4NReO_4 = 100/100/1.

complex **5** was also prepared using a one-pot procedure starting with tetrabutylammonium perrhenate and triphenylphosphane hydrochloride in dichloromethane (entry 4, Table 1).

These examples illustrate a new strategy for labeling estradiol ligands with rhenium using a solid-supported hydrazine substrate, and this chemistry should also be successful for preparing technetium analogs.[12] The ability to use perrhenate and pertechnetate salts for labeling is particularly advantageous, since these species are obtained directly from the radionuclide generators. The efficiency and convenience of this approach can be extrapolated to a new generation of rhenium and technetium complexes for diagnostic and therapeutic applications in nuclear medicine. Further studies that are currently in progress involve evaluation of the receptor binding affinity and in vivo stability of these estradiol derivatives, and the extension of this technology to other low-capacity receptor systems.

Experimental Section

4: To a suspension of Tentagel Carboxy resin (1.0 g, 0.26 mmol) in dichloromethane (50 mL) was added PyBOP (405 mg, 0.78 mmol) followed by hydrazine **3** and diisopropylethylamine (0.3 mL). The resulting suspension was stirred at 25 °C for 20 h. The reaction product was filtered to give the yellow polymer support **4**. FT-IR (KBr): $\tilde{\nu}$ = 3443, 2869, 1652, 1611, 1104 cm^{-1}.

5: A suspension of **4** (110 mg, 0.0286 mmol), triphenylphosphane (7.5 mg, 0.0286 mmol), and $[ReOCl_3(PPh_3)_2]$ (23.8 mg, 0.0286 mmol) in dichloromethane (10 mL) was heated at 40 °C for 3 h. The reaction mixture was filtered, and washed thoroughly with dichloromethane. The combined organic layers were concentrated, and the product was precipitated from dichloromethane/hexanes and recrystallized to provide the complex **5** (28 mg, 82 %) as olive-green crystals containing CH_2Cl_2. Elemental analysis for $C_{62}H_{57}Cl_3NO_2P_2Re \cdot 0.5\,CH_2Cl_2$: calcd: C 60.23, H 4.61, N 1.12; found: C 60.29, H 4.66, N 1.50. Spectral data is provided in the Supporting Information.

Received: September 13, 1999 [Z14014]

[1] Generator technology is available for producing $^{188}ReO_4^-$ and $^{99m}TcO_4^-$. a) S. C. Srivastava in *Current Directions in Radiopharmaceutical Research and Development* (Ed.: S. J. Mather), Kluwer Academic, Netherlands, **1996**, pp. 63–79; b) S. Mirzadeh, F. F. Knapp, Jr., *J. Radioanal. Nucl. Chem. Art.* **1996**, *203*, 471–488.
[2] W. C. Eckelman, *Eur. J. Nucl. Med.* **1995**, *22*, 249–263.
[3] R. K. Hom, J. A. Katzenellenbogen, *Nucl. Med. Biol.* **1997**, *24*, 485–498.
[4] J. R. Dilworth, S. J. Parrott, *Chem. Soc. Rev.* **1998**, *27*, 43–55.
[5] J. A. Katzenellenbogen, M. A. Welch, F. Dehdashti, *Anticancer Res.* **1997**, *17*, 1573–1576.
[6] S. Top, H. El Hafa, A. Vessières, J. Quivy, J. Vaissermann, D. W. Hughes, M. J. McGlinchey, J. P. Mornon, E. Thoreau, G. Jaouen, *J. Am. Chem. Soc.* **1995**, *117*, 8372–8380.
[7] F. Minutolo, J. A. Katzenellenbogen, *J. Am. Chem. Soc.* **1998**, *120*, 13264–13265.
[8] F. Wüst, K. E. Carlson, J. A. Katzenellenbogen, H. Spies, B. Johannsen, *Steroids* **1998**, *63*, 665–671.
[9] J. B. Arterburn, I. Fogarty, K. A. Hall, K. C. Ott, J. C. Bryan, *Angew. Chem.* **1996**, *108*, 3039–3040; *Angew. Chem. Int. Ed. Engl.* **1996**, *35*, 2877–2879.
[10] E. C. Lisic, S. Mirzadeh, F. F. Knapp, Jr., *J. Labelled Compd. Radiopharm.* **1993**, *33*, 65–75.
[11] a) S. Takahashi, Y. Kuroyama, K. Sonogashira, N. Hagihara, *Synthesis* **1980**, 627–630; b) F. Stieber, U. Grether, H. Waldmann, *Angew. Chem.* **1999**, *111*, 1142–1145; *Angew. Chem. Int. Ed.* **1999**, *38*, 1073–1077.
[12] a) T. Nicholson, A. Davison, J. A. Zubieta, Q. Chen, A. G. Jones, *Inorg. Chim. Acta* **1995**, *230*, 205–208; b) F. D. Rochon, R. Melanson, P. C. Kong, *Inorg. Chem.* **1995**, *34*, 2273–2277.

Regioselective Lactonization of Tetrasialic Acid**

Mou-Chi Cheng, Chun-Hung Lin,* Hsiu-Yin Wang, Heng-Ru Lin, and Shih-Hsiung Wu*

Polysialic acids (PSAs) are polymers of *N*-acetylneuraminic acid. Depending on their glycosidic linkages, these sugar polymers exist in nature as α-2,8-, α-2,9-, and α-2,8/2,9-linked polysaccharides.[1] PSAs have been reported to demonstrate many important biological functions.[2] For example, α-2,8-PSA is mainly linked to the neural cell adhesion molecule (N-CAM). This homopolymer of sialic acid has been implicated in reducing N-CAM adhesion; removal of the PSA increases the adhesive capability of N-CAM.[3] In addition, α-2,8- and α-2,9-PSAs are the capsular polysaccharides of, respectively, serogroups B and C of *Neisseria meningitidis*, a leading worldwide cause of meningitis and rapidly fatal sepsis in otherwise healthy individuals.[4]

Structural diversities of PSAs are even more complicated with the possibility of PSA lactonizations. For α-2,8-PSA, the C-2 carboxylic acid of one residue can condense with the C-9 hydroxyl group of an adjacent residue to generate a δ-lactone under acidic conditions. Such δ-lactonizations have also been

[*] Prof. Dr. S.-H. Wu,[+] Prof. Dr. C.-H. Lin, M.-C. Cheng, H.-Y. Wang, H.-R. Lin
Institute of Biological Chemistry
Academia Sinica, Taipei (Taiwan)
Fax: (+886) 2-2788-3473
E-mail: shwu@gate.sinica.edu.tw, chunhung@gate.sinica.edu.tw
[+] Additional Address:
Institute of Biochemical Sciences
National Taiwan University, Taipei (Taiwan)

[**] Financial support for this work was provided by the National Science Council of Taiwan and the Academia Sinica (Taiwan).

observed in α-2,8/2,9-PSA.[5] Some unusual properties of PSAs can be attributed to the occurrence of these PSA lactones. For instance, the formation of ganglioside lactones has been found in nature and was suggested to play an important biological role.[6] Moreover, in vivo lactonizations of the serogroup B PSA of *Neisseria meningitidis* are proposed to explain the poor immunogenicity shown in humans. In contrast, the serogroup C PSA of the same organism is a better immunogen since it is difficult for the α-2,9-homopolymer of the sialic acid to undergo lactonization due to the steric hindrance of the C8 hydroxyl group.[5, 7]

Recently, we have demonstrated the use of capillary electrophoresis (CE) for elucidating the lactonization of α-2,8-trisialic acid.[8] It was found that formation of the fully lactonized trimer occurred by the pathway in which monolactone **1** is the dominant intermediate (Scheme 1). The other monolactone **2** was the sole intermediate observed during the hydrolysis of the fully lactonized trimer. Meanwhile, it has been suggested by Zhang and Lee that initial lactonizations of α-2,8-oligosialic acids occur between internal sialic acid residues.[9] To further clarify whether regioselectivity exists in the lactonization of oligo/polysialic acids with a degree of polymerization (DP) greater than three and to compare lactonizations between different linkages of PSAs, we report here our investigations into α-2,8-tetrasialic acid and its 2,9-analogue.

α-2,8-Tetrasialic acid **3** was treated with glacial acetic acid to initiate lactonization which was then monitored by CE. As shown in Figure 1, six peaks in the CE chromatograms can be grouped into four categories (A to D). Peak A with the lowest mobility is the starting material, free tetrasialic acid (**3**); this was proved by co-injection with an authentic standard. Peak D is recognized as the fully lactonized tetramer **4** with the lowest charge density. Obviously, peaks A and D showed their predominant presence in the initial and final stages of lactonization, respectively (Stages 1) and 5) in Figure 1). Based on the retention times measured on CE chromatograms, it is reasonable to suggest that groups B and C correspond to the mono- and dilactonized species, respectively. These signals could not be identified without enzymatic

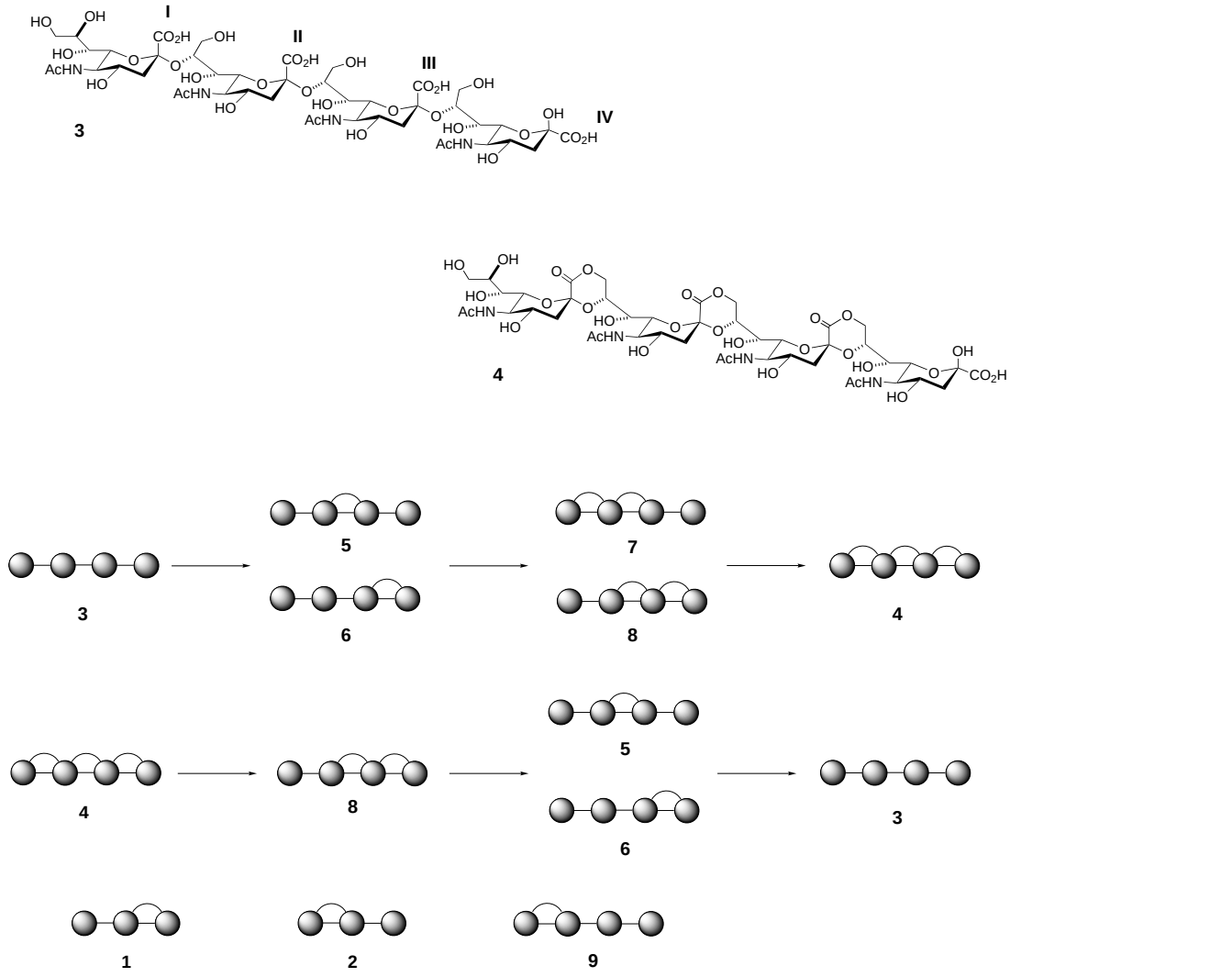

Scheme 1. Structures of α-2,8-linked sialic acid tetramer **3** and fully lactonized tetramer **4** as well as simplified representations of trimeric monolactones **1** and **2** and the reaction pathways of lactonization (upper) and delactonization (lower). Sialic acid residues are represented by the spheres; the reducing termini are always on the right side. Sites of lactone rings are marked by the curves between spheres. Compound **5** was the major monolactonized tetramer with **6** as the minor one in both pathways. The tetrameric monolactone **9** was not detected in the lactonization.

  0044-8249/00/11204-0789 $ 17.50+.50/0

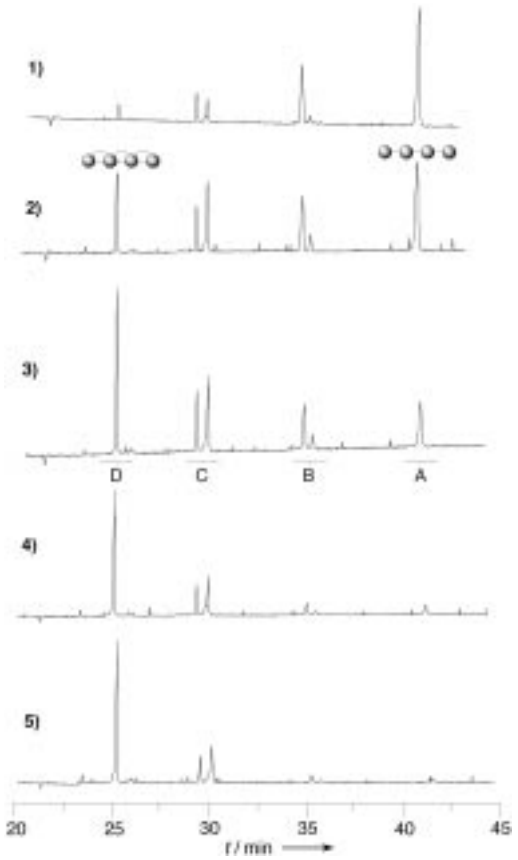

Figure 1. CE chromatograms of the lactonization of **3** in glacial acetic acid at different reaction times (Stage 1) = 10 min, 2) = 60 min, 3) = 3 h, 4) = 8 h, and 5) = 16 h).

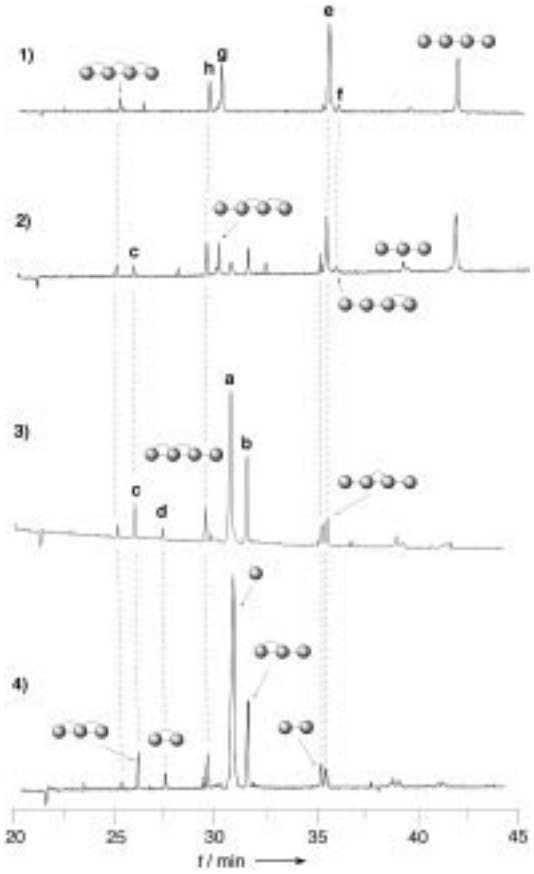

Figure 2. CE chromatograms of the hydrolysis of the mixed lactonization products by neuraminidase at different times of incubation (Stage 1) = 0 min, 2) = 10 min, 3) = 1 h, and 4) = 2 h).

hydrolysis by neuraminidase, the progress of which is depicted in Figure 2. Peaks a to d were identified as sialic acid monomer, trimeric monolactone **2**, fully lactonized trimer, and lactonized dimer, respectively, by co-injection studies and comparison of retention times with authentic standards.

The formation of **2** (peak b) and lactonized dimer (peak d) should result from the enzymatic cleavage of the tetrameric monolactones **5** and **6**, respectively, because neuraminidase cleaves sialic acid residues exclusively from the nonreducing end and stops when the sialic acid residue at the nonreducing end is lactonized. Due to the results of the enzymatic hydrolysis and the intensity changes of the peaks (Figure 2), peaks e and f (group B in Figure 1) are concluded to be the tetrameric monolactones **5** and **6**, which can be hydrolyzed by neuraminidase. Monolactones **5** and **6** can further lactonize to give the dilactonized tetramers as peaks g and h (group C in Figure 1. Peak h is identified as compound **7** because of its resistance to neuraminidase hydrolysis. Compound **8**, with the two consecutive lactone rings in the reducing terminal, is assigned to peak g due to its rapid disappearance by hydrolytic cleavage by neuraminidase. The hydrolysis of **8** results in the formation of the fully lactonized trimer, as shown by the appearance and increasing intensity of peak c. Based on the results illustrated in Figures 1 and 2, the lactonization pathway of the sialic acid tetramer can be deduced (Scheme 1). At first, the free tetramer **3** was lactonized to generate **5** as the major monolactone and **6** as the minor one. The monolactones were further lactonized to form dilactones **7** and **8**, respectively, and finally to form the fully lactonized tetramer **4**.

These results confirmed the previous proposal that the internal sialic acid residues in oligo/polysialic acids are more inclined to lactonize[9] since **5** was formed as the major product in the initial stage of lactonization. Our lactonization experiments were conducted in glacial acetic acid so all carboxylic acids should be in the protonated form. Inspection of the molecular structure of tetrasialic acid (**3**) indicates that the internal carboxylic acids (II and III, Scheme 1) confront more dipole–dipole repulsion than the external ones. Carboxylic acids II and III therefore have less freedom and this explains why they show more tendency to lactonize, which leads to the formation of **5** and **6**, respectively. Since the carboxylic acid in the reducing terminal (IV) is in the equatorial position due to the anomeric effect,[10] carboxylic acid II is expected to be more confined and easier to lactonize than III; this was proved by the observation that **5** was the predominant monolactone and **6** was formed in only trace quantities at the beginning of lactonization. On the other hand, the tetrameric monolactone **9** (Scheme 1) was undetected in our investigation. Such a result is consistent with the observation that lactone formation is faster at the reducing terminal than at the nonreducing end.

The fully lactonized tetramer **4** was treated with 0.05 M $(NH_4)_2CO_3$ to understand how it is hydrolyzed under alkaline conditions. As shown in Figure 3, the CE analysis indicated

  0044-8249/00/11204-0790 $ 17.50+.50/0

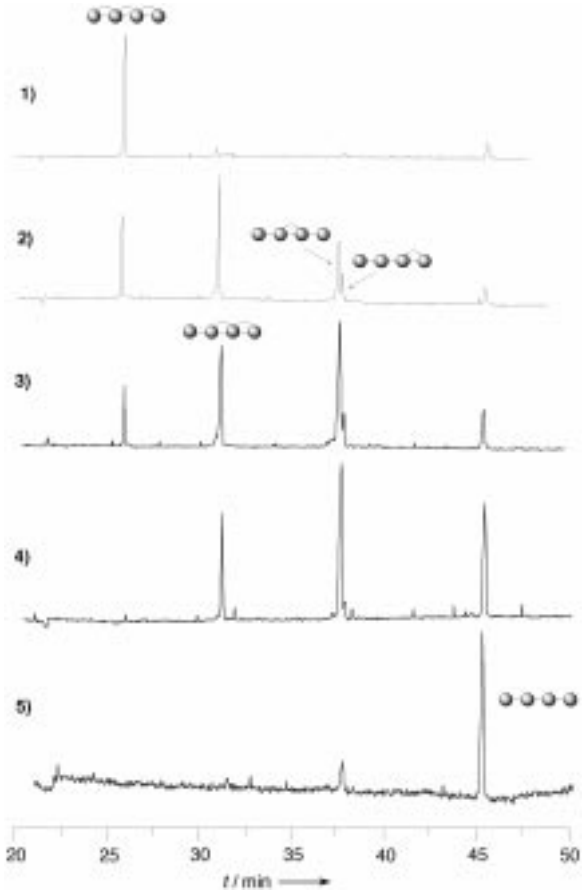

Figure 3. CE chromatograms of the hydrolysis of **4** under alkaline conditions at different reaction times (Stage 1) = 0 min, 2) = 10 min, 3) = 1 h, 4) = 4 h, and 5) = 16 h).

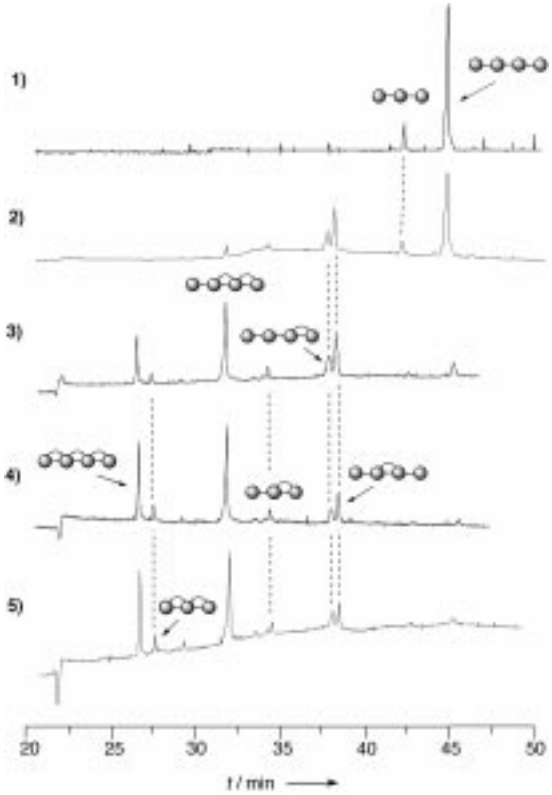

Figure 4. CE chromatograms of the lactonization of α-2,9-linked sialic acid tetramer in glacial acetic acid at different reaction times (Stage 1) = 0 day, 2) = 1 day, 3) = 2 days, 4) = 3 days, and 5) = 6 days). The tetramer was contaminated with a small amount of the trimer so that trimeric monolactone and dilactone were also observed. The structures of the α-2,9-linked sialic acid oligomers and lactonized species are equivalent to the α-2,8-linked species except for the glycosidic linkage.

that dilactone **8** was generated first and followed by the mixture of the two monolactones **5** and **6**, with **5** being produced preferentially. All the peak assignments were verified by co-injections of the samples from both lactonization and enzyme hydrolysis and further confirmed by mass spectrometry analyses. It was intriguing that the intensity ratio of two tetrameric monolactones changed as a function of hydrolytic times with **5** gradually becoming predominant. The different stabilities of the two monolactones under alkaline hydrolysis may reasonably explain this observation.

The same studies were carried out for α-2,9-tetrasialic acid. Except for the extremely slow rate of lactonization (Figure 4), similar patterns of lactone formation and hydrolysis were observed, which was not surprising based on our explanations mentioned above.

In comparison with a similar investigation using high performance anion-exchange chromatography, our analysis using CE affords a superior method with high resolution to identify each lactonized species as well as sialic acid oligomers. In fact, this is the first report to demonstrate the progress of lactonization of sialic acid oligomers and present clear evidence of the initial lactonization taking place at the internal positions. The study of lactonization of oligosialic acids could provide a better understanding of the natural lactonization of PSAs which may represent an on/off mechanism for a physiological function.[11]

Experimental Section

N-Acetylneuraminic acid tetramer ([→8Neu5Acα2→]$_4$) was obtained as the gift from Prof. Yasuo Inoue (Institute of Biological Chemistry, Academia Sinica, Taiwan) and NGK Biochemical Ltd. (Handa, Japan). Alpha-2,9-tetrasialic acid was isolated from meningococcal serogroup C and obtained from Prof. T.-Y. Liu (Institute of Biological Chemistry, Academia Sinica, Taiwan). Neuraminidase from *Anthrobacter ureafaciens* was purchased from Sigma (St. Louis, USA). The treatment of α-2,9-tetrasialic acid was the same as that of α-2,8-tetrasialic acid except for longer reaction times.

Lactonization of **3**: Free tetramer **3** (25 μg) was incubated in glacial acetic acid (1 mL) at room temperature. The reaction was stopped by freezing with liquid nitrogen and then dried immediately in a SpeedVac concentrator (Savant, USA) to remove acetic acid. Dried samples were dissolved in doubly distilled water and an aliquot (5 μL) of the mixture was analyzed by high performance capillary electrophoresis (HPCE).

Preparation of **4**: Free tetramer **3** (25 μg) was left in glacial acetic acid (1 mL) at room temperature for 8 h, frozen with liquid nitrogen, and then dried immediately in a SpeedVac concentrator (Savant, USA) to remove acetic acid.

Delactonization of **4**: Trilactone **4** (50 μg) was dissolved in 0.05 M ammonium carbonate (500 μL) at 37 °C. Aliquots were withdrawn at periods of 20, 40, and 80 min, frozen with liquid nitrogen, and then dried in a SpeedVac concentrator (Savant, USA). Dried samples were dissolved in doubly distilled water and an aliquot (5 μL) of the mixture was analyzed by HPCE.

Chromatographic Conditions: Capillary electrophoreses (CE) were performed on a Beckman capillary electrophoresis system (P/ACE 2100) using a fused silica capillary (118 cm×75 μm) and carried out by applying 20 kV

  0044-8249/00/11204-0791 $ 17.50+.50/0

at 25 °C. Phosphate buffer (50 mM, pH 8.0) was used as the running buffer. The chromatograms were monitored by UV absorption at 200 nm. Samples were injected into the capillary by high pressure nitrogen (20 psi) for 3 s. The capillary was regenerated by washing with 0.1M NaOH for 5 min after purging with doubly distilled water for 3 min.

Neuraminidase Hydrolysis: Partially lactonized samples (10 μg) in ammonium acetate buffer (100 mM, pH 5) were digested with neuraminidase (1 mU) from *Anthrobacter ureafaciens* in 20-μL CE vials at room temperature. The progress of hydrolysis was monitored at each time interval by HPCE.

Received: July 23, 1999 [Z13374]

[1] a) R. Yamasaki in *Polysialic acid: From Microbes to Man* (Eds: J. Roth, U. Rutishhauser, F. A. Troy II), Birkhäuser, Basel, **1993**, pp. 1–9; b) H. J. Jennings, J. R. Brisson, M. Kulakowska, F. Michon in *Polysialic acid: From Microbes to Man* (Eds.: J. Roth, U. Rutishhauser, F. A. Troy II), Birkhäuser, Basel, **1993**, pp. 25–38; c) M. Muhlenhoff, M. Eckhardt, R. Gerardy-Schahn, *Curr. Opin. Struct. Biol.* **1998**, *8*, 558–564; d) W. Egan, T.-Y. Liu, D. Dorow, J. S. Cohen, J. D. Robbins, E. C. Gotschlich, J. B. Robbins, *Biochemistry* **1977**, *16*, 3687–3692.

[2] a) U. Rutishhauser, L. Landmesser, *Trends Neurosci.* **1996**, *19*, 422–427; b) J. Z. Kiss, G. Rougon, *Curr. Opin. Neurobiol.* **1997**, *7*, 640–646; c) U. Rutishhauser, *Curr. Opin. Cell Biol.* **1996**, *8*, 679–684; d) H. Shen, M. Watanabe, H. Tomasiewicz, U. Rutishhauser, T. Magnuson, J. D. Glass, *J. Neurosci.* **1997**, *17*, 5221–5229.

[3] a) A. Acheson, J. L. Sunshine, U. Rutishhauser, *J. Cell Biol.* **1991**, *48*, 143–153; b) U. Rutishhauser in *Polysialic acid: From Microbes to Man* (Eds.: J. Roth, U. Rutishhauser, F. A. Troy II), Birkhäuser, Basel, **1993**, pp. 215–227.

[4] a) H. Baumann, J. R. Brisson, F. Michon, R. Pon, H. J. Jenning, *Biochemistry* **1993**, *32*, 4007–4013; b) J. Hayrinen, H. J. Jenning, H. V. Raff, G. Rougon, N. Hanai, R. Gerardy-Schahn, J. Finne, *J. Infect. Dis.* **1995**, *171*, 1481–1490.

[5] a) M. R. Lifely, A. S. Gilbert, C. Moreno, *Carbohydr. Res.* **1981**, 94, 193–203; b) M. R. Lifely, A. S. Gilbert, C. Moreno, *Carbohydr. Res.* **1984**, *134*, 229–243.

[6] a) S. K. Gross, M. A. Williams, R. H. McCluer, *J. Neurochem.* **1980**, *34*, 1351–1361; b) L. Riboni, S. Sonnino, D. Acquotti, A. Malesci, R. Ghidoni, H. Egge, I. Mingrino, G. Tettamanti, *J. Biol. Chem.* **1986**, *261*, 8514–8519; c) I. Kawashima, M. Kotani, H. Ozawa, M. Suzuki, T. Tai, *Int. J. Cancer* **1994**, *58*, 263–268; d) W. Kielczynski, R. K. Bartholomeusz, L. C. Harrison, *Glycobiology* **1994**, *4*, 791–796.

[7] H. J. Jennings, *Curr. Top. Microbiol. Immunol.* **1990**, *150*, 97–127.

[8] M.-C. Cheng, C.-H. Lin, K.-H. Khoo, S.-H. Wu, *Angew. Chem.* **1999**, *111*, 743–746; *Angew. Chem. Int. Ed.* **1999**, *38*, 686–689.

[9] Y. Zhang, C. Y. Lee, *J. Biol. Chem.* **1999**, *274*, 6183–6189.

[10] "The Anomeric Effect and Associated Stereoelectronic Effects": G. R. J. Thatchen, *ACS Symp. Ser.* **1993**, *539*, chap. 2.

[11] a) R. K. Yu, T. A. W. Koerner, S. Ando, H. C. Yohe, J. H. Prestegard, *J. Biochem.* **1985**, *98*, 1367–1373; b) B. Maggio, T. Agria, R. K. Yu, *Biochemistry* **1990**, *29*, 8729–8734.

Octahedral Coordination of an Iodide Ion in an Electrophilic Sandwich**

Hans Lee, Martin Diaz, Carolyn B. Knobler, and M. Frederick Hawthorne*

Until now, no discrete six-coordinate iodide (−1 oxidation state) sandwich species has been reported. A limited number of octahedral complexes such as $[I^{VII}F_6]^+$,[1] $[I^{VII}(OH)_6]^+$,[2] and $[I^{V}F_6]^-$[3] (distorted octahedral) with iodine in a formal +7 or +5 oxidation state are known. Multidentate Lewis acidic hosts form four- to six-coordinate iodine species, with iodine in a formal −1 oxidation state.[4, 5] The field of anion host–guest chemistry offers prospects for molecular recognition, anion transport, and catalysis.[4–6]

Penta-, tetra-, and tridentate organomercury receptors form complexes with halide anions and a variety of neutral electron-rich species. The cyclic pentameric $[(CF_3)_2CHg]_5$ coordinates two halide anions (Cl^-, Br^-, I^-), one above and one below the center of the cavity.[7, 8] Similarly, tetrameric 12-mercuracarborand-4 $(C_2B_{10}H_{10}Hg)_4$ can also bind two iodide ions, while the smaller chloride and bromide ions usually reside within the cavity to produce 1:1 host–guest complexes.[9] Trimeric perfluoro-*o*-phenylenemercury coordinates halide ions in a 1:1 stoichiometric ratio of trimer:halide. The halide ions are situated above and below the cavity to form an infinite bent polydecker structure with the composition $[(o\text{-}C_6F_4Hg)_3X]^-$ (X = Cl, Br, I) and a distorted octahedral geometry around the anion.[8, 10]

Here we report the synthesis and structural characterization of the first discrete octahedral sandwich complex $[\mathbf{1}_2 \cdot I]^-$, composed of two electroneutral trimeric *B*-hexamethyl-9-mercuracarborand-3 $[9,12\text{-}(CH_3)_2\text{-}C_2B_{10}H_8Hg]_3$ (**1**) receptors which simultaneously coordinate an iodide ion in a sandwich fashion.

The reaction of LiI with **1** results in the sandwich complex $[\mathbf{1}_2 \cdot I]^-$ in 82% yield. $Li[\mathbf{1}_2 \cdot I]$ is an air- and moisture-stable crystalline solid. The ^1H, ^{13}C, and ^{11}B NMR spectra revealed that $[\mathbf{1}_2 \cdot I]^-$ has a highly symmetrical structure, with chemical shifts nearly identical to those of the empty host **1**.[11] The ^{199}Hg NMR spectrum of $[\mathbf{1}_2 \cdot I]^-$ in acetone exhibits a singlet at $\delta = -957$, with no evidence of the empty host **1** ($\delta = -1158$).[11] A downfield shift relative to the signal of **1** is diagnostic of coordination of a guest to the mercury atoms of **1**.[9] The ^{199}Hg NMR chemical shifts of similar complexes of organomercury compounds exhibit strong dependencies on the nature of the solvent and the concentration of the complex.[12] $Li[\mathbf{1}_2 \cdot I]$ has a ^{199}Hg NMR chemical shift which is essentially independent of concentration at room temperature. This observation suggests that the solid-state structure of $Li[\mathbf{1}_2 \cdot I]$ is maintained in solution.[9] The negative-ion fast atom bombardment (FAB) mass spectrum exhibits a peak centered at m/z 2351, with the

[*] Prof. Dr. M. F. Hawthorne, H. Lee, M. Diaz, Dr. C. B. Knobler
Department of Chemistry and Biochemistry
University of California at Los Angeles
Los Angeles, CA 90095 (USA)
Fax: (+1) 310-825-5490
E-mail: mfh@chem.ucla.edu

[**] This work was supported by the National Science Foundation.

  0044-8249/00/11204-0792 $ 17.50+.50/0